

SeqFormer: a Frustratingly Simple Model for Video Instance Segmentation

Junfeng Wu^{1*} Yi Jiang² Wenqing Zhang^{1*} Xiang Bai^{1†} Song Bai²

¹Huazhong University of Science and Technology ²ByteDance

Abstract

In this work, we present *SeqFormer*, a frustratingly simple model for video instance segmentation. *SeqFormer* follows the principle of vision transformer that models instance relationships among video frames. Nevertheless, we observe that a stand-alone instance query suffices for capturing a time sequence of instances in a video, but attention mechanisms should be done with each frame independently. To achieve this, *SeqFormer* locates an instance in each frame and aggregates temporal information to learn a powerful representation of a video-level instance, which is used to predict the mask sequences on each frame dynamically. Instance tracking is achieved naturally without tracking branches or post-processing. On the YouTube-VIS dataset, *SeqFormer* achieves 47.4 AP with a ResNet-50 backbone and 49.0 AP with a ResNet-101 backbone without bells and whistles. Such achievement significantly exceeds the previous state-of-the-art performance by 4.6 and 4.4, respectively. In addition, integrated with the recently-proposed Swin transformer, *SeqFormer* achieves a much higher AP of 59.3. We hope *SeqFormer* could be a strong baseline that fosters future research in video instance segmentation, and in the meantime, advances this field with a more robust, accurate, neat model. The code and the pre-trained models are publicly available at <https://github.com/wjf5203/SeqFormer>.

1. Introduction

Video Instance Segmentation (VIS) [26] is an emerging vision task that aims to simultaneously perform detection, classification, segmentation, and tracking of object instances in videos. Compared to image instance segmentation [6], video instance segmentation is much more challenging since it requires accurate tracking of objects across an entire video.

Previous VIS algorithms can be roughly divided into two

* Work done during an internship at ByteDance AI Lab.

† Corresponding author.

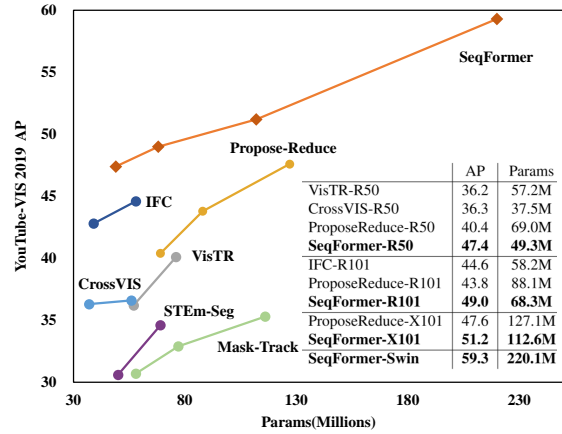


Figure 1. **Performance vs. Model Size.** All results are reported with single model and single-scale inference. *SeqFormer* significantly outperforms the previous method with similar parameters.

categories. The first mainstream follows the tracking-by-detection paradigm, extending image instance segmentation models with a tracking branch [3, 13, 26, 27]. These methods first predict candidate detection and segmentation frame-by-frame, and then associate them by classification [27, 27] or re-identification [3, 13] to track the instance through a video. However, the tracking process is sensitive to occlusions and motion blur that are common in videos. Another mainstream predicts clip-level instance masks by taking a video clip [1, 2] or the entire video [8, 24] as input. It divides a video into multiple overlapping clips and generates mask sequences with clip-by-clip matching on overlapping frames. Recently, VisTR [24] adapts transformer [22] to VIS and uses instance queries to obtain instance sequence from video clips. After that, IFC [8] improves the performance and efficiency by building communications between frames in a transformer encoder.

In this paper, we present Sequential Transformer (*SeqFormer*), which follows the principle of vision transformer [4, 24] and models instance relationships among video frames. As in [8], we observe that a stand-alone instance query suffices although an object may be of different positions, sizes, shapes, and various appearances. Neverthe-

less, it is witnessed that the attention process shall be done with each frame independently, so that the model will attend to locations following the movement of instance through the video. This observation aligns with the conclusion drawn in action recognition [17, 28], in which the 1D time domain and 2D space domain have different characteristics and should be handled in a different fashion.

Considering the movement of an instance in a video, a model is supposed to attend to different spatial locations following the motion of the instance. We decompose the shared instance query into frame-level box queries for the attention mechanism to guarantee that the attention focuses on the same instance on each frame. The box queries are kept on each frame and used to predict the bounding box sequences. Then the features within the bounding boxes are aggregated to refine the box queries on the current frame. By repeating this refinement process through decoder layers, SeqFormer locates the instance in each frame in a coarse-to-fine manner, in a similar way to Deformable DETR [29].

However, to mitigate redundant information from non-instance frames, those box queries are aggregated in a weighted manner, where the weights are learned upon the box embeddings. The generated representation, which retains richer object cues, is used to predict the category and generate dynamic convolution weights of mask head. Since the box sequences are predicted and refined in the decoder, SeqFormer naturally and succinctly establishes the association of instances across frames.

In summary, SeqFormer enjoys the following advantages:

- SeqFormer is a neat and simple end-to-end framework. Given an arbitrary long video as input, SeqFormer predicts the classification results, box sequences, and mask sequences in one step without the need for additional tracking branches or hand-craft post-processing.
- As shown in Fig. 1, SeqFormer sets the new state-of-the-art performance on YouTube-VIS 2019 benchmark [26]. SeqFormer achieves 47.4 AP with a ResNet-50 backbone and 49.0 AP with a ResNet-101 backbone without bells and whistles. Such achievement significantly exceeds the previous state-of-the-art performance by 4.6 and 4.4, respectively. With a ResNext-101 backbone, SeqFormer achieves 51.2 AP, which is the first time that an algorithm achieves an AP above 50. In addition, integrated with the recently-proposed Swin transformer, SeqFormer achieves a much higher AP of 59.3.
- With the query decomposition mechanism, SeqFormer attends to locations following the movement of instance through the video and learns a powerful representation for instance sequences.

- The code and the pre-trained models are publicly available. We hope the SeqFormer, with the idea of making attention follow the movement of object, could be a strong baseline that fosters future research in video instance segmentation, and in the meantime, advances this field with a more robust, accurate, neat model.

2. Related Work

Image Instance Segmentation Instance Segmentation is the most fundamental and challenging task in computer vision, which aims to detect every instance and segment every pixel respectively in static images. Instance segmentation was dominated by Mask R-CNN [6] for a long time, Mask R-CNN [6] directly introduces fully convolutional mask head to Faster R-CNN [18] in a multi-task learning manner. Recently, one stage models emerged as excellent frameworks for instance segmentation. Solo [23] and CondInst [20] propose one stage instance segmentation pipeline and achieve comparable performance. CondInst [20] proposes to dynamically generate the mask head parameters for each instance, which is used to predict the mask of the corresponding instance. Dynamic mask head can be efficiently adopted into video segmentation tasks because the same instance in different frames can share the same mask head.

Video Instance Segmentation. Video instance segmentation is extended from the traditional image instance segmentation, and aims to simultaneously segment and track all object instances in the video. The baseline method MaskTrack R-CNN [26] is built upon Mask R-CNN [6] and introduces a tracking head to associate each instance in the video. Sip-Mask [3] follows the similar pipeline based on the one-stage FCOS [21]. MaskProp [2] introduces a mask propagation module that propagates instance masks from each video frame to all the other frames in a video clip, which can improve the segmentation performance and compute clip-level instance tracks. However, the temporal receptive field of a clip modeling is limited by the length of the input clip without having a global view from the whole video. CrossVIS [27] proposes a new learning scheme that uses the instance feature in the current frame to pixel-wisely localize the same instance in other frames. Propose-Reduce [10] introduces a new paradigm that adds an extra sequence propagation across frames head upon Mask R-CNN [6], which can achieve high performance, but it is very computationally intensive.

Transformers. Transformer [22] was first proposed for the sequence-to-sequence machine translation task and became the basic component in most Natural Language Processing tasks. Recently, Transformers [22] has been successfully applied in many visual tasks. DETR [4] proposes a new detection paradigm upon transformers, which simplifies the traditional detection framework and abandons

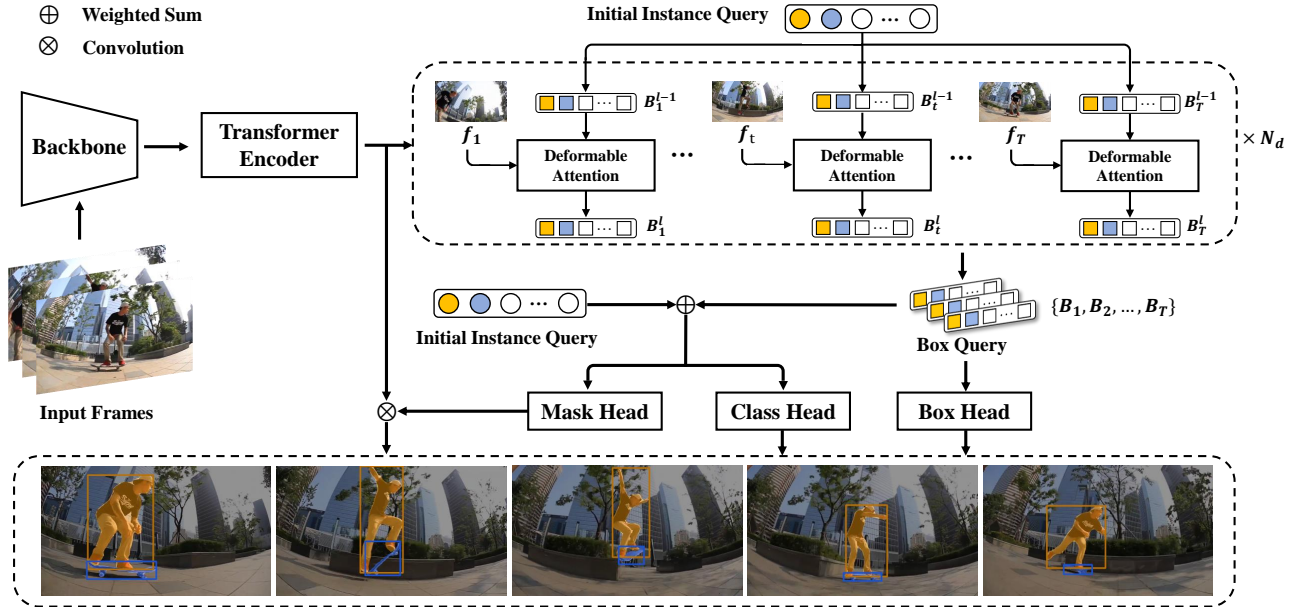


Figure 2. The overall architecture of SeqFormer. Given the feature maps of input frames, the initial instance query is decomposed into frame-level box queries at the first decoder layer. The box queries are kept on each frame and serve as anchors without interacting with each other. The features extracted by box queries from each frame are aggregated to the instance query after each decoder layer, which is used for predicting dynamic mask head weight. Then the mask head convolves the encoded feature map to generate the mask sequences.

the hand-crafted post-processing module. Deformable Detr [29] achieves better performance by using local attention and multi-scale feature maps. VisTR [24] is the first method that adapts DETR [4] to the VIS task and uses instance queries to obtain instance sequence from video clips. However, VisTR can not handle variable-length or long-time video sequences due to the fixed number of input queries hardcoded with video length. IFC [8] improves the performance and efficiency of VisTR by building communications between frames in the transformer encoder instead of flattening the space-time features into one dimension. However, both of them still flatten the space-time features for the transformer decoder. Our model is designed to carry out the instance feature capturing independently on different frames, which makes the model attend to locations following the movement of instance through the video.

3. Method

3.1. Architecture

The network architecture is visualized in Fig. 2. SeqFormer has a CNN backbone and a transformer encoder for extracting feature maps from each frame independently. Next, a transformer decoder is adapted to locate the instance sequences and generate a video-level instance representation. Finally, three output heads are used for instance classification, instance sequences segmentation, and bounding

box prediction, respectively.

Backbone Given an input video $x_v \in \mathbb{R}^{T \times 3 \times H \times W}$ with 3 color channels and T frames of resolution $H \times W$, the CNN backbone (e.g., ResNet [7]) extracts feature maps for each frame independently.

Transformer Encoder First, a 1×1 convolution is used to reduce the channel dimension of the all the feature maps to $C = 256$, creating new feature maps $\{\mathbf{f}'_t\}_{t=1}^T, \mathbf{f}'_t \in \mathbb{R}^{C \times H' \times W'}, t \in [1, T]$. After adding fixed positional encodings [4], the transformer encoder performs deformable attention [29] on the feature maps, resulting in the output feature maps $\{\mathbf{f}_t\}_{t=1}^T$, with the same resolutions as the input. To perform attention mechanisms on each frame independently, we keep the spatial and temporal dimensions of feature maps rather than flattening them into one dimension.

Query Decompose Transformer Decoder Given a video, humans can effortlessly identify every instance and associate them through the video, despite the various appearance and changing positions on different frames. If an instance is hard to recognize due to occlusion or motion blur in some frames, humans can still re-identify it through the context information from other frames. In other words, for the same instance on different frames, humans treat them as a whole instead of individuals. This is the crucial difference between video and image instance segmentation. Motivated by this, we propose Query Decompose Transformer

Decoder, which aims to learn a more and robust video-level instance representation across frames.

We introduce a fixed number of learnable embeddings to query the features of the same instance from each frame, termed Instance Queries. Different from the instance queries corresponding to frame-level instances in VisTR [24], our instance queries correspond to video-level instances. Since the changing appearance and position of the instance, the model should focus on different exact spatial locations of each frame. To achieve this goal, we propose to decompose the instance query into T frame-specific box queries, each of which serves as an anchor for retrieving and locating features on the corresponding frame.

At the first decoder layer, an instance query $\mathbf{I}_q \in \mathbb{R}^C$ is used to query the instance features on features maps of each frame independently:

$$\mathbf{B}_t^1 = \text{DeformAttn}(\mathbf{I}_q, \mathbf{f}_t), \quad (1)$$

where $\mathbf{B}_t^1 \in \mathbb{R}^C$ is the box query on frame t from the 1-st decoder layer, and DeformAttn indicates deformable attention module in [29]. Given a query element and the frame feature map \mathbf{f}_t , deformable attention only attends to a small set of key sampling points. At the l -th ($l > 1$) layer, the box query \mathbf{B}_t^{l-1} from last layer is used as input:

$$\mathbf{B}_t^l = \text{DeformAttn}(\mathbf{B}_t^{l-1}, \mathbf{f}_t), \quad (2)$$

and the instance query aggregates the temporal features by a weighted sum of all the box queries, where the weights are end to end learned upon the box embedding:

$$\mathbf{I}_q^l = \frac{\sum_{t=1}^T \mathbf{B}_t^l \times \text{FC}(\mathbf{B}_t^l)}{\sum_{t=1}^T \text{FC}(\mathbf{B}_t^l)} + \mathbf{I}_q^{l-1}. \quad (3)$$

After N_d decoder layers, we get an instance query and T box queries for each instance. The instance query is a shared video-level instance representation, and the box query contains the position information for predicting the bound box on each frame. The N instance queries are transformed into an output instance embedding and T box embeddings $\{\mathbf{BE}_t\}_{t=1}^T$, $\mathbf{BE}_t \in \mathbb{R}^{N \times d}$.

Output Heads As shown in Fig. 2, we add mask head, box head, class head on the top of the decoder outputs. A linear projection acts as the class head to produce the classification results. Given the instance embedding from the transformer decoder with index $\sigma(i)$, class head output a class probability of class c_i (which may be \emptyset) as $\hat{p}_{\sigma(i)}(\mathbf{c}_i)$.

The box head is a 3-layer feed forward network (FFN) with ReLU activation function and a linear projection layer. For \mathbf{BE}_t of each frame, the FFN predicts the normalized center coordinates, height and width of the box w.r.t. the frame. Thus, for the instance with index $\sigma(i)$, we denote the predicted box sequence as $\hat{\mathbf{b}}_{\sigma(i)} =$

$\{\hat{\mathbf{b}}_{(\sigma(i),1)}, \hat{\mathbf{b}}_{(\sigma(i),2)}, \dots, \hat{\mathbf{b}}_{(\sigma(i),T)}\}$. Since instance embedding contains the information of instance on all frames, it can be regarded as a more robust instance representation. We can use instance embedding to efficiently generate the entire mask sequences. To this end, we leverage dynamic convolution as mask head. First, a 3-layer FFN encodes the instance embedding into parameters ω_i of mask head with index $\sigma(i)$, which has three 1×1 convolution layers. Each convolution layer has 8 channels and uses ReLU as the activation function except for the last one, following [20].

As shown in Fig. 2, there is a mask branch that provides the feature maps for mask head to predict instance masks. We employ an FPN-like architecture to make the use of multi-scale feature maps from transformer encoder and generate feature maps sequences $\{\hat{\mathbf{F}}_{\text{mask}}^1, \hat{\mathbf{F}}_{\text{mask}}^2, \dots, \hat{\mathbf{F}}_{\text{mask}}^T\}$ that are $\frac{1}{8}$ of the input resolution and have 8 channels for each frame independently. Then the feature map $\hat{\mathbf{F}}_{\text{mask}}^t$ is concatenated with a map of the relative coordinates from center of $\hat{\mathbf{b}}_{(\sigma(i),t)}$ in corresponding frames to provide a location cue for predicting the instance mask. Thus we get the $\{\mathbf{F}_{\text{mask}}^t\}_{t=1}^T$, $\mathbf{F}_{\text{mask}}^t \in \mathbb{R}^{10 \times \frac{H}{8} \times \frac{W}{8}}$. The sequence feature maps $\mathbf{F}_{\text{mask}}^t$ is sent to the mask head to predict the mask sequences:

$$\{\mathbf{m}_i^t\}_{t=1}^T = \{\text{MaskHead}(\mathbf{F}_{\text{mask}}^t, \omega_i)\}_{t=1}^T, \quad (4)$$

where MaskHead performs three-layer 1×1 convolution on given feature maps with the kernels reshaped from ω . By sharing the same mask head, our method can efficiently perform instance segmentation on each frame. Similar to DETR [4], we add output heads and Hungarian loss after each decoder layer as an auxiliary loss to supervise the training stage. All output heads share their parameters.

3.2. Instance Sequences Matching and Loss

Our method predicts a fixed-size set of N predictions in a single pass through the decoder, and N is set to be significantly larger than the number of instances in a video. To train our network, we first need to find a bipartite graph matching between the prediction and the ground truth. Let \mathbf{y} denotes the ground truth set of video-level instance, and $\hat{\mathbf{y}}_i = \{\hat{\mathbf{y}}_i\}_{i=1}^N$ denotes the predicted instance set. Each element i of the ground truth set can be seen as $\mathbf{y}_i = \{\mathbf{c}_i, (\mathbf{b}_{i,1}, \mathbf{b}_{i,2}, \dots, \mathbf{b}_{i,T})\}$, where \mathbf{c}_i is the target class label including \emptyset , and $\mathbf{b}_{i,t} \in [0, 1]^4$ is a vector that defines ground truth bounding box center coordinates and its relative height and width in the frame t . For the predictions of instance with index $\sigma(i)$, we take the output of class head $\hat{p}_{\sigma(i)}(\mathbf{c}_i)$ and predicted bounding box $\hat{\mathbf{b}}_{\sigma(i)}$. Then we define the pair-wise matching cost between ground truth y_i and a prediction with index $\sigma(i)$.

$$\mathcal{L}_{\text{match}}(\mathbf{y}_i, \hat{\mathbf{y}}_{\sigma(i)}) = -\hat{p}_{\sigma(i)}(\mathbf{c}_i) + \mathcal{L}_{\text{box}}(\mathbf{b}_i, \hat{\mathbf{b}}_{\sigma(i)}), \quad (5)$$

where $\mathbf{c}_i \neq \emptyset$.

Note that Eq. (5) does not consider the similarity between mask prediction and mask ground truth, as such mask-level comparison is computationally expensive. To find the best assignment of a ground truth to a prediction, we search for a permutation of N elements $\sigma \in S_n$ with the lowest cost:

$$\hat{\sigma} = \arg \min_{\sigma \in S_n} \sum_i^N \mathcal{L}_{\text{match}}(\mathbf{y}_i, \hat{\mathbf{y}}_{\sigma(i)}). \quad (6)$$

Following prior work [4, 24], the optimal assignment is computed with the Hungarian algorithm [9]. Given the optimal assignment $\hat{\sigma}$, we use Hungarian loss for all matched pairs to train our network:

$$\mathcal{L}_{\text{Hung}}(\mathbf{y}, \hat{\mathbf{y}}) = \sum_{i=1}^N \left[-\log \hat{p}_{\hat{\sigma}(i)}(\mathbf{c}_i) + \mathbb{1}_{\{\mathbf{c}_i \neq \emptyset\}} \mathcal{L}_{\text{box}}(\mathbf{b}_i, \hat{\mathbf{b}}_{\hat{\sigma}(i)}) + \mathbb{1}_{\{\mathbf{c}_i \neq \emptyset\}} \mathcal{L}_{\text{mask}}(\mathbf{m}_i, \hat{\mathbf{m}}_{\hat{\sigma}(i)}) \right]. \quad (7)$$

For \mathcal{L}_{box} , we use a linear combination of the \mathcal{L}_1 loss and the generalized IoU loss [19]. The mask sequences $\{m_i^t\}_{t=1}^T$ from mask head with $\frac{1}{8}$ of the video resolution which may lose some details, thus we upsample the predicted mask to $\frac{1}{4}$ of the video resolution, and downsample the ground truth mask to the same resolution for mask loss, following [20]. The mask loss $\mathcal{L}_{\text{mask}}$ is defined as a combination of the Dice [16] and Focal loss [11]. We calculate box loss and mask loss on each frame and take the average for Hungarian loss.

4. Experiment

4.1. Datasets and Metrics

We evaluate our method on YouTube-VIS 2019 [26] and YouTube-VIS 2021 [25] datasets. YouTube-VIS 2019 is the first and largest dataset for video instance segmentation, which contains 2238 training, 302 validation, and 343 test high-resolution YouTube video clips. It has a 40-category label set and 131k high-quality instance masks. In each video, objects with bounding boxes and masks are labeled every five frames. YouTube-VIS 2021 is an improved and extended version of YouTube-VIS 2019 dataset, it contains 3,859 high-resolution videos and 232k instance annotations. The newly added videos in the dataset include more instances and frames.

Video instance segmentation is evaluated by the metrics of average precision (AP) and average recall (AR). Different from image instance segmentation, each instance in a video contains a sequence of masks. To evaluate the spatio-temporal consistency of the predicted mask sequences, the IoU computation is carried out in the spatial-temporal domain. This requires a model not only to obtain accurate seg-

mentation and classification results at frame-level but also to track instance masks between frames accurately.

4.2. Implementation Details

Model settings ResNet-50 [7] is used as our backbone network unless otherwise specified. Similar to [29], we use the features from the last three stages as {C3, C4, C5} in ResNet, which correspond to the feature maps with strides {8, 16, 32}. And adding the lowest resolution feature map C6 obtained via a 3×3 stride 2 convolution on the C5. We set sampled key numbers $K=4$ and eight attention heads for deformable attention modules. We use six encoder and six decoder layers of hidden dimension 256 for the transformer, and the number of instance queries is set to 300.

Training We used AdamW [15] optimizer with base learning rate of 2×10^{-4} , $\beta_1 = 0.9$, $\beta_2 = 0.999$, and weight decay of 10^{-4} . Learning rates of the backbone and linear projections used for deformable attention modules are multiplied by a factor of 0.1. We first pre-train the model on COCO [12] by setting the number of input frames $T = 1$. Given the pretrained weights, we train our models on the YouTube-VIS dataset with input frames $T = 5$ sampled from the same video.

The training data of the YouTube-VIS dataset is not sufficient, which makes a model prone to overfitting. To address this problem, we adopt 80K training images in the COCO for compensation, following [1, 10]. We only use the images with 20 overlapping categories in COCO and augment them with $\pm 10^\circ$ rotation to generate a five-frame pseudo video. We train our model on the mixed dataset including COCO and the video dataset for 12 epochs, and the learning rate is decayed at the 6-th and 10-th epoch by a factor of 0.1. The input frame sizes are downsampled so that the longest side is at most 768 pixels. The model is implemented with PyTorch-1.7 and is trained on 8 V100 GPUs of 32G RAM, with 2 video clips per GPU.

Inference SeqFormer is able to model a video of arbitrary length without grouping frames into subsequences. We take the whole video as input during inference, which is down-scaled to 360p, following MaskTrack R-CNN [26]. SeqFormer learns a video-level instance representation used for dynamic segmentation on each frame and classification, and the box sequences are generated in the decoder. Thus, no post-processing is needed for associating instances.

4.3. Main Results

The comparison of SeqFormer with previous state-of-the-art methods on YouTube-VIS 2019 are listed in Table 1. MaskProp [2] and ProposeReduce [10] are the state-of-the-art methods, which take a strong backbone to extract spatial features and use mask propagation to improve the segmentation and tracking, but suffer from low inference speed.

Backbone	Method	Params	AP	AP ₅₀	AP ₇₅	AR ₁	AR ₁₀
ResNet-50	MaskTrack R-CNN [26]	58.1M	30.3	51.1	32.6	31.0	35.5
	STEm-Seg [1]	50.5M	30.6	50.7	33.5	37.6	37.1
	SipMask [3]	33.2M	33.7	54.1	35.8	35.4	40.1
	CompFeat [5]	-	35.3	56.0	38.6	33.1	40.3
	SG-Net [13]	-	34.8	56.1	36.8	35.8	40.8
	VisTR [24]	57.2M	36.2	59.8	36.9	37.2	42.4
	MaskProp [2]	-	40.0	-	42.9	-	-
	CrossVIS [27]	37.5M	36.3	56.8	38.9	35.6	40.7
	Propose-Reduce [10]	69.0M	40.4	63.0	43.8	41.1	49.7
	IFC [8]	39.3M	42.8	65.8	46.8	43.8	51.2
	SeqFormer	49.3M	47.4	69.8	51.8	45.5	54.8
ResNet-101	MaskTrack R-CNN [26]	77.2M	31.8	53.0	33.6	33.2	37.6
	STEm-Seg [1]	69.6M	34.6	55.8	37.9	34.4	41.6
	SG-Net [13]	-	36.3	57.1	39.6	35.9	43.0
	VisTR [24]	76.3M	40.1	64.0	45.0	38.3	44.9
	MaskProp [2]	-	42.5	-	45.6	-	-
	CrossVIS [27]	56.6M	36.6	57.3	39.7	36.0	42.0
	Propose-Reduce [10]	88.1M	43.8	65.5	47.4	43.0	53.2
	IFC [8]	58.3M	44.6	69.2	49.5	44.0	52.1
		SeqFormer	68.4M	49.0	71.1	55.7	46.8
ResNeXt-101	MaskProp [2]	-	44.3	-	48.3	-	-
	Propose-Reduce [10]	127.1M	47.6	71.6	51.8	46.3	56.0
	SeqFormer	112.7M	51.2	75.3	58.0	46.5	57.3
Swin-L	SeqFormer	220.0M	59.3	82.1	66.4	51.7	64.4

Table 1. Quantitative results of video instance segmentation on YouTube-VIS 2019 validation set. The best results with the same backbone are in **bold**.

We list the methods with different backbones for fair comparison. It can be observed that SeqFormer significantly surpasses all the previous best reported results by at least 4 AP with the same backbone. SeqFormer with a ResNet-50 backbone can even achieve competitive performance against state-of-the-art methods with a ResNeXt-101 backbone. By adopting Swin transformer [14] as our backbone without further modifications, SeqFormer can first achieve 59.3 AP on this benchmark, outperforming the best previous results by a large margin of 11.7 AP. In Fig. 3, we visualize the results of SeqFormer with four challenging cases. It can be seen that SeqFormer can handle these situations well. We also evaluate our approach on the recently introduced YouTube-VIS 2021 dataset, which is a more challenging dataset with more videos and a higher number of instances and frames. As shown in Table 2, SeqFormer achieves 40.5 AP with a ResNet-50 backbone, surpassing previous methods by 3.9 AP. We believe that our effective method will serve as a strong baseline on these benchmarks and facilitate future research in video instance segmentation.

Method	AP	AP ₅₀	AP ₇₅	AR ₁	AR ₁₀
MaskTrack	28.6	48.9	29.6	26.5	33.8
SipMask	31.7	52.5	34.0	30.8	37.8
CrossVIS	34.2	54.4	37.9	30.4	38.2
IFC	36.6	57.9	39.3	-	-
SeqFormer	40.5	62.4	43.7	36.1	48.1
SeqFormer-S	51.8	74.6	58.2	42.8	58.1

Table 2. Quantitative results on YouTube-VIS 2021 validation set. We use a ResNet-50 as backbone for all the experiment expect Swin transformer for SeqFormer-S.

4.4. Ablation Study

This section conducts extensive ablation experiments to study the effects of different settings in our proposed method. All the ablation experiments are conducted with the ResNet-50 backbone and training on YouTube-VIS 2019 dataset rather than the mixed dataset.

Instance query decomposition Instance query decomposition plays an important role in our method. Since an in-

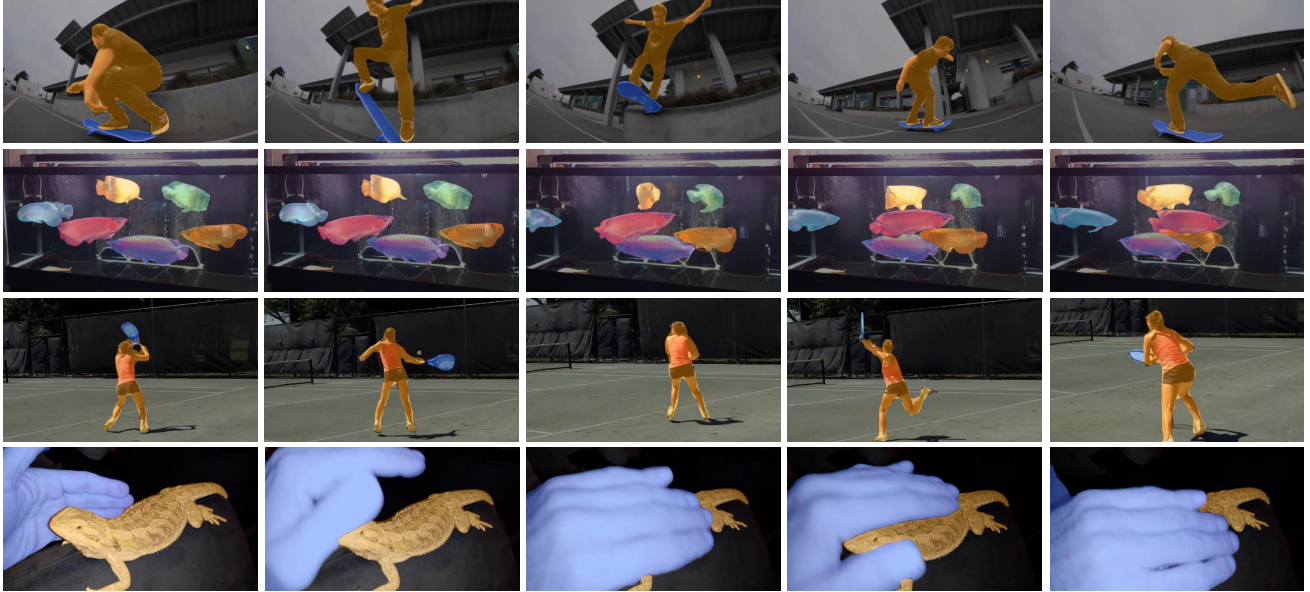


Figure 3. Visualization of SeqFormer on the YouTube-VIS 2019 [26] validation dataset. The first row shows the instances with various poses. The second row shows the case of a lot of similar instances that are close together with overlapping. The third row shows the situation where an instance reappears after being occluded while in motion. The last row shows an instance severely occluded by the other instance. The same colors depict the mask sequences of the same instances

Decompose	AP	AP ₅₀	AP ₇₅	AR ₁	AR ₁₀
w/o	34.1	53.7	34.9	34.8	40.9
w	45.1	66.9	50.5	45.6	54.6

Table 3. Instance query decomposition. Decomposing instance query into frame-level box queries is critical for SeqFormer.

stance may have different positions on each frame, the iterative refinement of the spatial sampling region should be performed independently on each frame. To keep the temporal consistency of instances, we use the temporal-shared instance query for deformable attention and get box queries for each frame. The box queries will be kept through all the decoder layers and serve as frame anchors for the same instance. Experiments of models without box queries and using the shared instance query for each decoder layer are presented in Table 3. The model without query decomposition manages to achieve only 34.1 AP. It is because the query controls the sampling region of deformable attention. Using the same instance query for each frame will result in the same spatial sampling region on each frame, as shown in Fig. 4 (a), which is inaccurate and insufficient for video-level instance representation. We further visualize the sampling points of the second and the last decoder layers in Fig. 4 (b) and (c). The box queries decoupled from instance query serve as anchors for locating features and iteratively refining the sampling region on the current frame. It can be seen that SeqFormer attends to locations following the

Feature	AP	AP ₅₀	AP ₇₅	AR ₁	AR ₁₀
flatten	35.1	56.8	35.6	38.1	41.8
single-scale	42.5	64.6	46.5	41.5	50.9
multi-scale	45.1	66.9	50.5	45.6	54.6

Table 4. Spatial and temporal dimensions. Keeping spatial-temporal feature dimensions and performing instance feature capture independently on different frames brings about 7.4 AP gains. Multi-scale feature maps can further bring 2.6 AP.

movement of instance through the video in a coarse-to-fine manner. Please refer to the Sup. Mat. for more visualization of sampling points.

Spatial and temporal dimensions Previous transformer-based methods [8, 24] flatten the spatial and temporal dimensions of video features into one dimension for the transformer decoder. We argue that the temporal dimension should not be flattened with spatial dimensions, since it was recognized that the 2D space domain and 1D time domain have different characteristics and should be intuitively handled in a different way [28]. Thus, we retain the complete 3D spatio-temporal dimensions and perform explicit region sampling and information aggregation on all frames. In this experiment, we study the effect of this architecture by replacing deformable transformer with vanilla transformer and flattening the spatial and temporal dimensions, termed as ‘flatten’ in Table 4. For fair comparison, we use

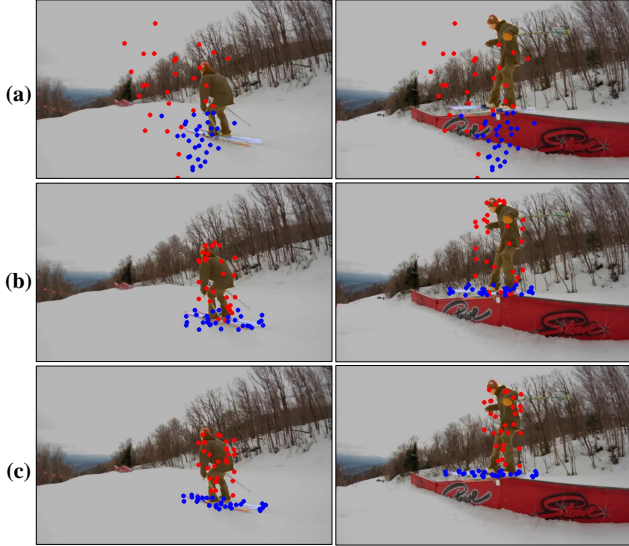


Figure 4. The sampling points from the first decoder layer is shown in (a), which is coarse and inaccurate. The refined accurate sampling points from the second and last decoder layer are shown in (b) and (c).

single-scale deformable attention as the baseline, termed as ‘single-scale’, which use the same scale feature map with ‘flatten’, the default setting termed as ‘multi-scale’. By keeping spatial-temporal dimensions of video features, the AP increased from 35.1 to 42.5. The use of multi-scale feature maps can only improve 2.6 AP, which proves that the success of our method mainly comes from the preservation of the temporal dimension and the explicit spatial sampling.

Aggregation of temporal information The frame-level box queries and the predicted boxes can align the instance features from all frames, there are several ways to aggregate the aligned features into the instance query. We conduct an experiment to evaluate the different aggregation ways for these features, as shown in Table 5. In the ‘sum’ setting, the features from different frames are directly added together as the instance feature of this decoder layer. In the ‘average’ setting, the feature on each frame is averaged as the instance feature. In the ‘weighted-sum’ setting, we apply a softmax layer and a fully-connected layer on box embeddings to get the weights of each frame, and the features are aggregated in a weighted sum in Eq. (3). The result is 30.6 AP and 43.2 AP for ‘sum’ and ‘average’ settings respectively. Direct summation will cause the value to be unstable with different frame numbers. Since some instances only appear in a few frames, directly averaging features from all frames may cause the information to be diluted. Please refer to the Sup. Mat. for more details and visualization of different frame weights.

Robust instance representation Our decoder explicitly

Aggregation	AP	AP ₅₀	AP ₇₅	AR ₁	AR ₁₀
sum	30.6	44.5	34.3	37.2	45.0
average	43.2	65.2	48.5	43.4	52.8
weighted-sum	45.1	66.9	50.5	45.6	54.6

Table 5. Temporal information aggregation. Weighted sum brings a performance gain of 1.9 in AP.

Frames	AP	AP ₅₀	AP ₇₅	AR ₁	AR ₁₀
1	38.1	58.3	41.3	38.7	47.5
3	43.4	65.4	47.6	42.4	51.3
5	44.6	66.5	49.7	44.8	54.6
10	44.7	66.9	49.5	44.3	53.5
all	45.1	66.9	50.5	45.6	54.6

Table 6. Fewer frames for instance representation. We evenly sample fewer frames from a video to generate the mask head.

aligns and aggregates the information from each frame to learn a video-level instance representation. In this experiment, we try to generate instance representation with fewer frames. To evaluate the instance representation, we use it to generate a mask head and apply mask head on each frame to get the mask sequences, as shown in Table 6. Surprisingly, with only one frame as input, the generated mask head can produce a competitive result of 38.1 AP. With five frames as input, the performance is only 0.5 AP worse than taking all frames as input. This result shows that the mask head learned by our method can generalize well to unseen frames.

4.5. Limitation

SeqFormer takes the entire video as input to generate the segmentation results of all frames in one step, so it cannot be directly applied to the online segmentation scenario.

5. Conclusion

In this paper, we have proposed an effective transformer architecture for video instance segmentation, named SeqFormer, which performs attention mechanisms on each frame independently and learns a shared powerful instance query for each video-level instance. With the proposed instance query decomposition, our network can align the instance features and naturally tackle the instance tracking without additional tracking branches or post-processing. We demonstrated that our method surpasses all state-of-the-art methods by a large margin. We believe that our simple yet effective approach will serve as a strong baseline for future research in video instance segmentation.

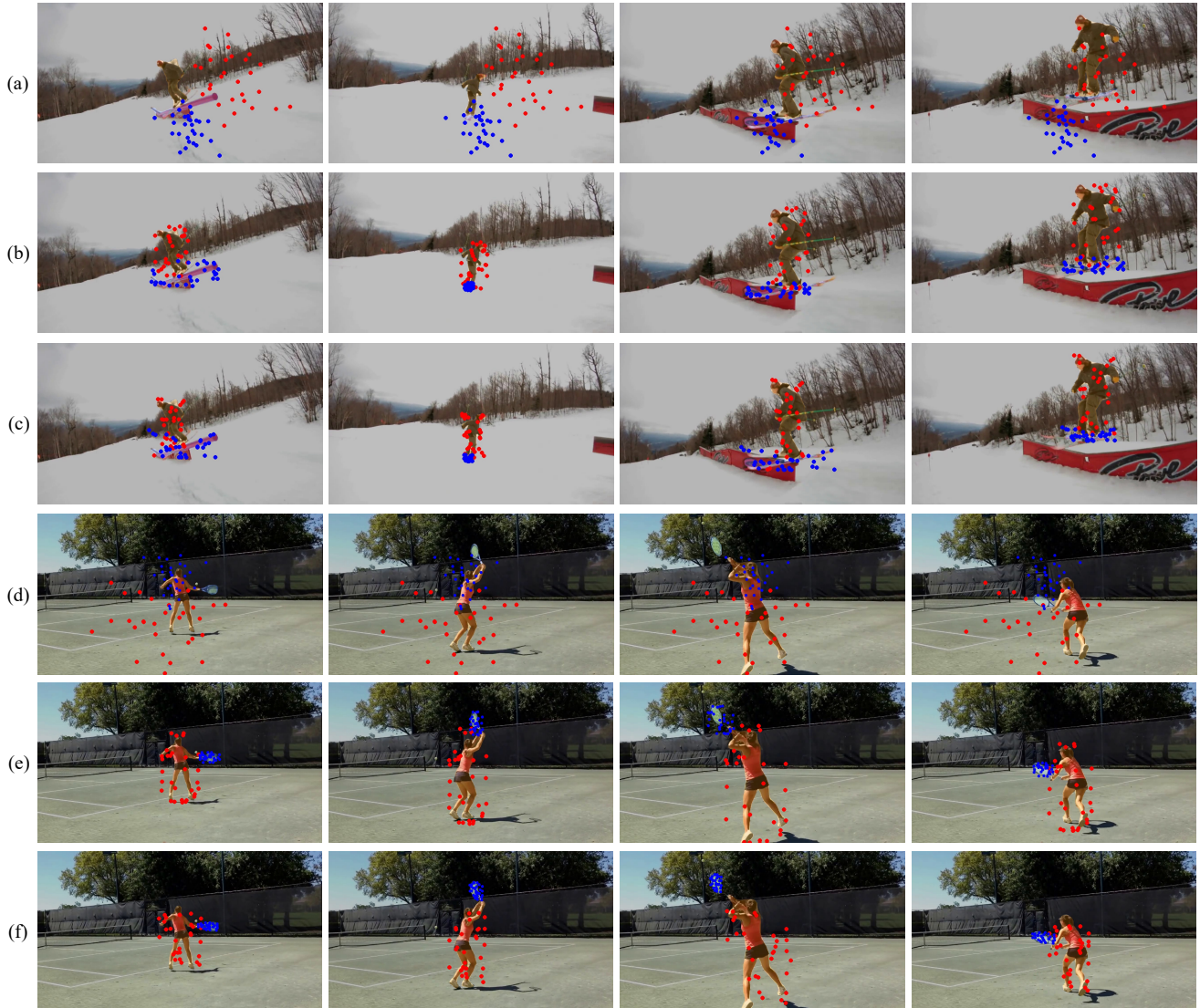


Figure 5. Visualization of attention. We draw the sampling points that the deformable attention attends to. The four frames in each row are from the same video. Each sampling point is marked as a filled circle whose color indicates its corresponding instance. (a) and (d) show the sampling points from the first decoder layer. (b) and (e) show the sampling points from the second decoder layer. (c) and (f) show the sampling points from the last decoder layer.

Appendix

Visualization of Attention

In Fig. 5, we show more qualitative results of the intermediate attention of transformer decoder. Since the same initial instance query is used to predict sampling points for each frame in the first decoder layer as show in Eq. (1), the distribution of sampling points on each frame is the same in Fig. 5(a) and (d). After that, the initial instance query is decomposed into frame-level box queries that are kept and maintained independently on each frame. Starting from the

second layer of the SeqFormer decoder, the box query is used to predict the sampling points of the current frame, and the sampled features are used to refine the box query for the next decoder layer. By doing so, SeqFormer attends to different spatial locations following the motion of the instance in a coarse-to-fine manner.

Aggregation of Temporal Information

SeqFormer is able to attend to different spatial locations following the motion of the instance. The aligned features are aggregated into an instance query to generate a video-level

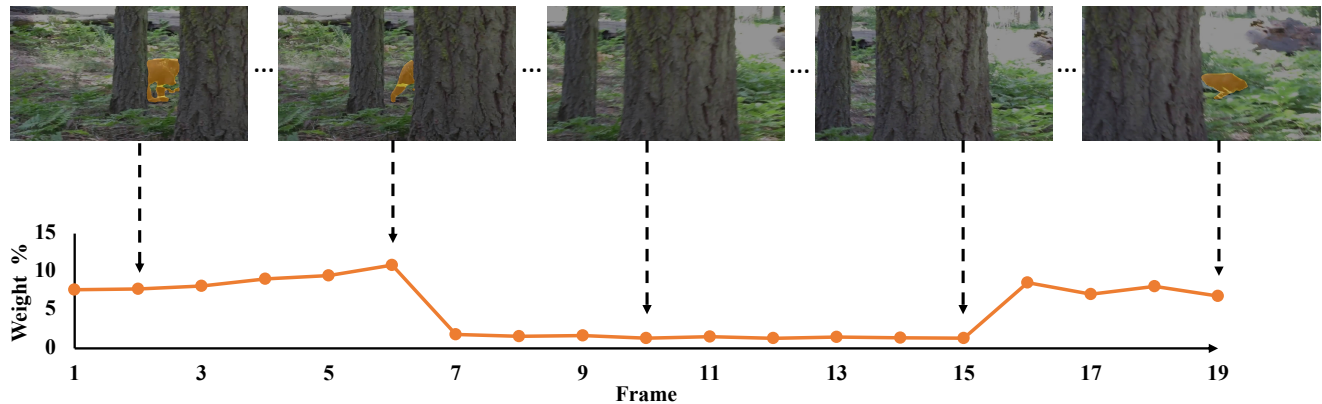


Figure 6. Visualization of the normalized softmax weights and the corresponding frames.

instance representation. However, an instance may not appear in every frame due to occlusion and camera motion. The features from frames without instance are useless or even harmful. To address this, SeqFormer aggregates temporal features in a weighted manner, where the weights are learned upon the box queries in Eq. (3). We visualize the learned weights and the corresponding frames in Fig. 6. It can be seen that the features from frames without instance have lower weights.

References

- [1] Ali Athar, Sabarinath Mahadevan, Aljosa Osep, Laura Leal-Taixé, and Bastian Leibe. Stem-seg: Spatio-temporal embeddings for instance segmentation in videos. In *ECCV*, 2020. 1, 5, 6
- [2] Gedas Bertasius and Lorenzo Torresani. Classifying, segmenting, and tracking object instances in video with mask propagation. In *CVPR*, 2020. 1, 2, 5, 6
- [3] Jiale Cao, Rao Muhammad Anwer, Hisham Cholakkal, Fahad Shahbaz Khan, Yanwei Pang, and Ling Shao. Sipmask: Spatial information preservation for fast image and video instance segmentation. In *ECCV*, 2020. 1, 2, 6
- [4] Nicolas Carion, Francisco Massa, Gabriel Synnaeve, Nicolas Usunier, Alexander Kirillov, and Sergey Zagoruyko. End-to-end object detection with transformers. In *ECCV*, 2020. 1, 2, 3, 4, 5
- [5] Yang Fu, Linjie Yang, Ding Liu, Thomas S Huang, and Humphrey Shi. Compfeat: Comprehensive feature aggregation for video instance segmentation. *arXiv preprint arXiv:2012.03400*, 2020. 6
- [6] Kaiming He, Georgia Gkioxari, Piotr Dollar, and Ross Girshick. Mask R-CNN. In *ICCV*, 2017. 1, 2
- [7] Kaiming He, Xiangyu Zhang, Shaoqing Ren, and Jian Sun. Deep residual learning for image recognition. In *CVPR*, 2016. 3, 5
- [8] Sukjun Hwang, Miran Heo, Seoung Wug Oh, and Seon Joo Kim. Video instance segmentation using inter-frame communication transformers. *arXiv preprint arXiv:2106.03299*, 2021. 1, 3, 6, 7
- [9] Harold W Kuhn. The hungarian method for the assignment problem. *Naval research logistics quarterly*, 2(1-2):83–97, 1955. 5
- [10] Huaijia Lin, Ruizheng Wu, Shu Liu, Jiangbo Lu, and Jiaya Jia. Video instance segmentation with a propose-reduce paradigm. *arXiv preprint arXiv:2103.13746*, 2021. 2, 5, 6
- [11] Tsung-Yi Lin, Priya Goyal, Ross Girshick, Kaiming He, and Piotr Dollár. Focal loss for dense object detection. In *ICCV*, 2017. 5
- [12] Tsung-Yi Lin, Michael Maire, Serge Belongie, James Hays, Pietro Perona, Deva Ramanan, Piotr Dollár, and C Lawrence Zitnick. Microsoft coco: Common objects in context. In *ECCV*, 2014. 5
- [13] Dongfang Liu, Yiming Cui, Wenbo Tan, and Yingjie Chen. Sg-net: Spatial granularity network for one-stage video instance segmentation. In *CVPR*, 2021. 1, 6
- [14] Ze Liu, Yutong Lin, Yue Cao, Han Hu, Yixuan Wei, Zheng Zhang, Stephen Lin, and Baining Guo. Swin transformer: Hierarchical vision transformer using shifted windows. *arXiv preprint arXiv:2103.14030*, 2021. 6
- [15] Ilya Loshchilov and Frank Hutter. Decoupled weight decay regularization. In *ICLR*, 2019. 5
- [16] Fausto Milletari, Nassir Navab, and Seyed-Ahmad Ahmadi. V-net: Fully convolutional neural networks for volumetric medical image segmentation. In *2016 fourth international conference on 3D vision (3DV)*, 2016. 5
- [17] Mandela Patrick, Dylan Campbell, Yuki M Asano, Ishan Misra, Florian Metze, Christoph Feichtenhofer, Andrea Vedaldi, Jo Henriques, et al. Keeping your eye on the ball: Trajectory attention in video transformers. *arXiv preprint arXiv:2106.05392*, 2021. 2
- [18] Shaoqing Ren, Kaiming He, Ross Girshick, and Jian Sun. Faster r-cnn: Towards real-time object detection with region proposal networks. In *NIPS*, 2015. 2
- [19] Hamid Rezaatofghi, Nathan Tsoi, JunYoung Gwak, Amir Sadeghian, Ian Reid, and Silvio Savarese. Generalized intersection over union: A metric and a loss for bounding box regression. In *CVPR*, 2019. 5

- [20] Zhi Tian, Chunhua Shen, and Hao Chen. Conditional convolutions for instance segmentation. In *ECCV*, 2020. 2, 4, 5
- [21] Zhi Tian, Chunhua Shen, Hao Chen, and Tong He. FCOS: Fully convolutional one-stage object detection. In *ICCV*, 2019. 2
- [22] Ashish Vaswani, Noam Shazeer, Niki Parmar, Jakob Uszkoreit, Llion Jones, Aidan N Gomez, Łukasz Kaiser, and Illia Polosukhin. Attention is all you need. In *NIPS*, 2017. 1, 2
- [23] Xinlong Wang, Tao Kong, Chunhua Shen, Yuning Jiang, and Lei Li. Solo: Segmenting objects by locations. In *ECCV*, 2020. 2
- [24] Yuqing Wang, Zhaoliang Xu, Xinlong Wang, Chunhua Shen, Baoshan Cheng, Hao Shen, and Huaxia Xia. End-to-end video instance segmentation with transformers. In *CVPR*, 2021. 1, 3, 4, 5, 6, 7
- [25] Ning Xu, Linjie Yang, Jianchao Yang, Dingcheng Yue, Yuchen Fan, Yuchen Liang, and Thomas S. Huang. Youtube-vis dataset 2021 version. <https://youtube-vos.org/dataset/vis/>. 5
- [26] Linjie Yang, Yuchen Fan, and Ning Xu. Video instance segmentation. In *ICCV*, 2019. 1, 2, 5, 6, 7
- [27] Shusheng Yang, Yuxin Fang, Xinggang Wang, Yu Li, Chen Fang, Ying Shan, Bin Feng, and Wenyu Liu. Crossover learning for fast online video instance segmentation. *arXiv preprint arXiv:2104.05970*, 2021. 1, 2, 6
- [28] Yue Zhao, Yuanjun Xiong, and Dahua Lin. Trajectory convolution for action recognition. In *NIPS*, 2018. 2, 7
- [29] Xizhou Zhu, Weijie Su, Lewei Lu, Bin Li, Xiaogang Wang, and Jifeng Dai. Deformable detr: Deformable transformers for end-to-end object detection. *arXiv preprint arXiv:2010.04159*, 2020. 2, 3, 4, 5